THE BELL SYSTEM TECHNICAL JOURNAL
Vol. 56, No. 8, October 1977
Printed in U.S.A.

A Quasioptical Feed System for Radioastronomical Observations at Millimeter Wavelengths

By P. F. GOLDSMITH

(Manuscript received March 1, 1977)

We describe a quasioptical feed system for use with a 7-meter Cassegrain antenna at millimeter wavelengths. This system is designed to take full advantage of low noise, broadband mixer receivers and will be used for radioastronomical observations at frequencies between 60 GHz and 140 GHz. Two offset parabolic mirrors couple the radiation from the f/D = 5.7 antenna into the receiver feedhorn. A Fabry-Perot resonator operating at oblique incidence is used to inject the local oscillator energy into the signal path and to suppress response at the image frequency. The loss of the Fabry-Perot diplexer is 0.25 dB for the signal, while the coupling loss between the mixer waveguide flange and the main lobe of the antenna pattern should be ≤1 dB.

I. INTRODUCTION

For optimal use of an antenna for radio astronomy at millimeter wavelengths, the feed system should provide a number of functions and must satisfy a variety of stringent performance criteria. These include

(*i*) Low loss for the signal over an instantaneous bandwidth of ≥500 MHz.

(*ii*) A well-controlled antenna illumination pattern which should remain unchanged over as large a range of frequencies as possible.

(*iii*) A provision for making accurate absolute calibrations of the receiver gain and atmospheric attenuation—both of these require suppression of the image frequency response in systems incorporating mixers.

(*iv*) A facility for antenna beam switching at a rapid rate to minimize the sky-noise contribution to receiver noise.

(*v*) Since mixers are currently the dominant type of receiver at

frequencies between 60 GHz and 300 GHz, it would be advantageous to include local oscillator injection as part of the feed system if this can be done with low loss.

The present feed system has been designed to satisfy all of the preceeding requirements. In Section II we describe the feed system optics and analyze the measurements of system performance. In Section III we discuss various aspects of the Fabry-Perot diplexer including bandwidth, image rejection, local oscillator noise suppression, and loss for the signal and for the local oscillator. In Section IV we discuss the calibration system.

II. FEED SYSTEM OPTICS

2.1 Antenna

This feed system is designed to operate with the recently completed Bell Lahoratories millimeter antenna located at Holmdel, N.J. The antenna is an offset Cassegrain with a diameter of 7 meters and a f/D ratio of 5.7. The overall surface accuracy is approximately 0.01 cm rms, allowing operation with a moderately high beam efficiency at frequencies as high as 300 GHz. The main advantage of the offset Cassegrain design is that there is zero aperture hlockage, and a very low reflection coefficient and low sidelobe levels can be achieved.[1]

2.2 Gaussian beam theory

We shall discuss the feed system optics in terms of the propagation of a single gaussian mode. As discussed by Arnaud,[2] a gaussian beam propagating in free space has a power distribution perpendicular to the direction of propagation (taken to be the z axis) of the form

$$\frac{P(r)}{P(\mathrm{o})} = e^{-[r/\xi(z)]^2} \tag{1}$$

The beam half-width (radius) ξ depends on z, the distance along the axis of propagation, as

$$\xi^2(z) = \xi_o^2 + \left(\frac{z}{k_o \xi_o}\right)^2 \tag{2}$$

where ξ_o is the minimum beam half-width (heam waist radius), taken to be located at $z = 0$, and $k_o = 2\pi/\lambda$. The asymptotic angle of beam half-width growth is seen from eq (2) to be

$$\theta_\xi = 1/k_o \xi_o \tag{3}$$

Equations (1) to (3) apply to gaussian beams of infinite transverse extent. In any practical system the beam will be truncated at some level,

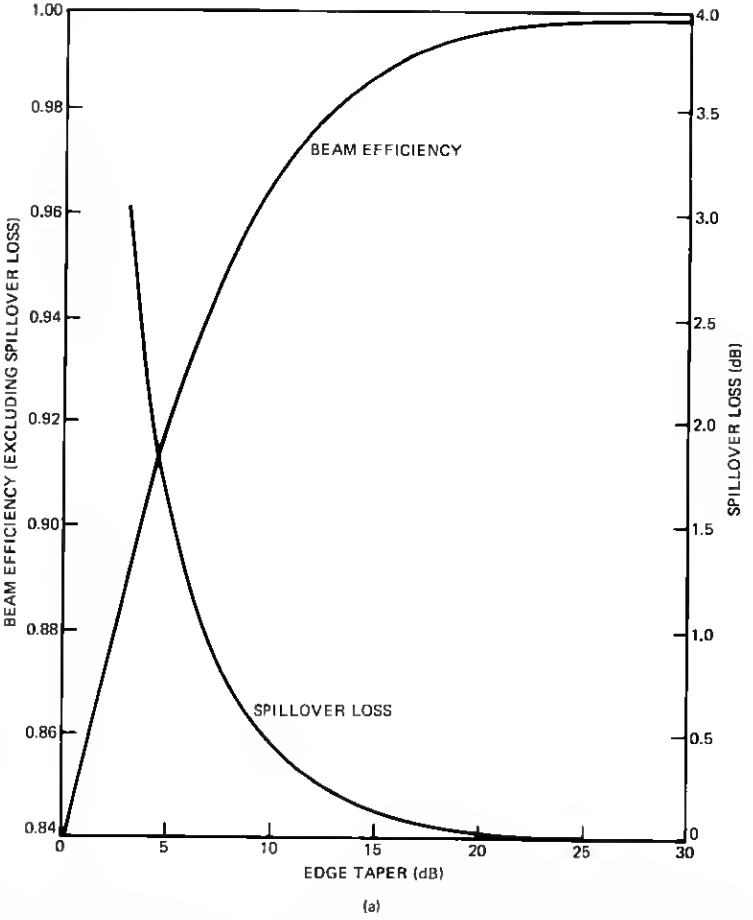

Fig. 1—(a) Beam efficiency and spillover loss for an unblocked, ideal antenna with gaussian aperture illumination, as a function of the edge taper. The edge taper is defined as the power density at the center of the antenna divided by the power density at the edge of the antenna. (b—next page) Beamwidth (full width at half maximum) for the same conditions. The radius of the antenna is a, and $k_0 = 2\pi/\lambda$.

which will produce sidelobes. In considering at what level the beam at the main reflector should be truncated, we have to balance consideration of spillover loss, sidelobe levels, and beam efficiency[3] against those of beamwidth and on-axis gain. Figure 1a shows the spillover loss and beam efficiency while Fig. 1b shows the beamwidth as a function of edge taper for an antenna with a gaussian aperture illumination pattern. The edge taper is defined as the power density at the center of the antenna divided by the power density at the edge. We have chosen an edge taper T_M close to 14 dB as being a satisfactory compromise. All other optical elements in the feed system truncate the beam at a much lower level (at least 23

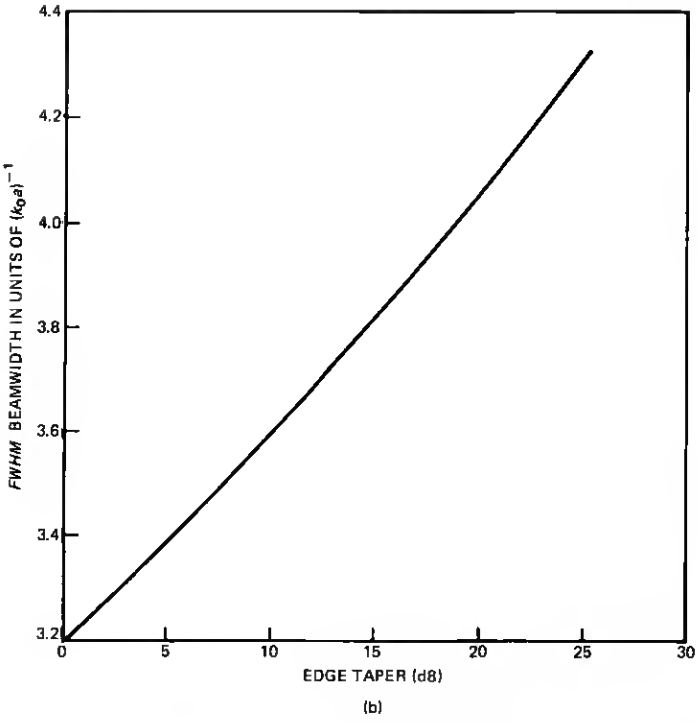

Fig. 1. (*continued from previous page*)

dB below the on-axis power level). We will thus ignore the effects of beam truncation within the feed system.

The edge taper at the main reflector is related to ξ_A, the antenna illumination beam half-width, by the formula

$$\xi_A = a\sqrt{\frac{10}{T \ln 10}} \tag{4}$$

where a is the main reflector radius (350 cm for this antenna) and T is the edge taper in decibels. We find that $\xi_A = 195$ cm for $T = 14$ dB. Since ξ_A is much larger than ξ_o, eq. (2) reduces to

$$\xi_A \approx z_A \theta_\xi = \frac{f}{k_o \xi_o} \tag{5}$$

where f is the focal length of the antenna (3955 cm). The resulting value for ξ_o at 100 GHz is 0.97 cm.

2.3 Feed system components

The large f/D ratio and resulting large beam waist size of the antenna makes coupling to the antenna beam waist directly with a feedhorn

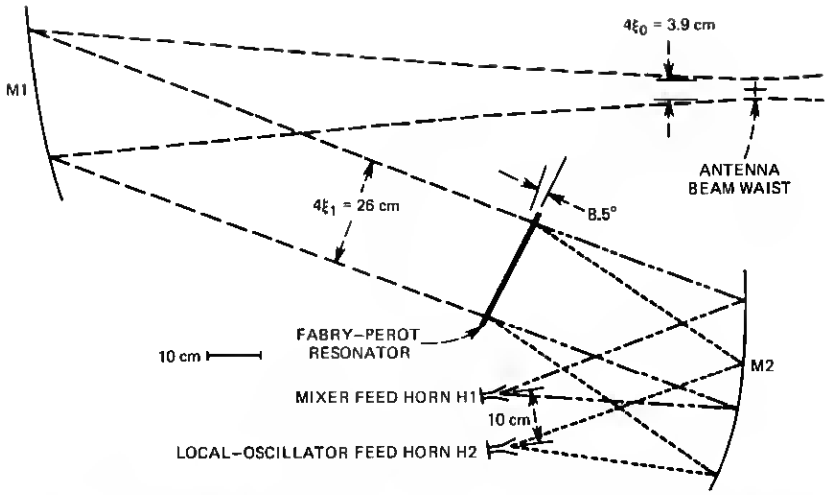

Fig. 2—Feed system optics. M1 and M2 are offset paraboloids. The diplexing action of the Fabry-Perot resonator (tilted 8.5 degrees from normal incidence) is shown schematically.

undesirable, especially for cryogenic receivers. Horn-lens arrangements were investigated but the losses involved were felt to be a significant disadvantage, especially when operation over very large bandwidths is required. In view of these facts, and also because of the desirability of an even larger beam waist size required for low loss in the Fabry-Perot diplexer (Section III), a feed system using metal mirrors is preferable. The arrangement of the feed system components is shown in Fig. 2. The overall size of the feed system is dictated by the beam waist size and the desire to minimize the number of mirrors involved.

Mirrors M1 and M2 are offset paraboloids; the offset angle for M1 is 20 degrees and the focal length is 136 cm. For M2 the offset angle is 30 degrees for the signal beam and the focal length is 44 cm. Offset antennas of this type have been shown to have excellent beam patterns.[4] The mirrors used in this work were cut on a numerically controlled milling machine; the peak deviation from the desired surface contour is approximately 0.05 mm.

The beam from the antenna expands until it reaches M1; at this point the beam half-width, denoted ξ_1, is 6.5 cm and is essentially frequency-independent. The distance from the beamwaist to M1 is equal to the focal length of the mirror so that in the geometrical optics limit the resulting beam would be collimated. The diffraction effects in the beam between M1 and M2 are small; in actuality a second beam waist is created in the large beam at a distance equal to the focal length from M1. Ideally, the separation between M1 and M2 would be equal to the sum of their focal lengths (180 cm) but a calculation[5] of the mismatch due to the

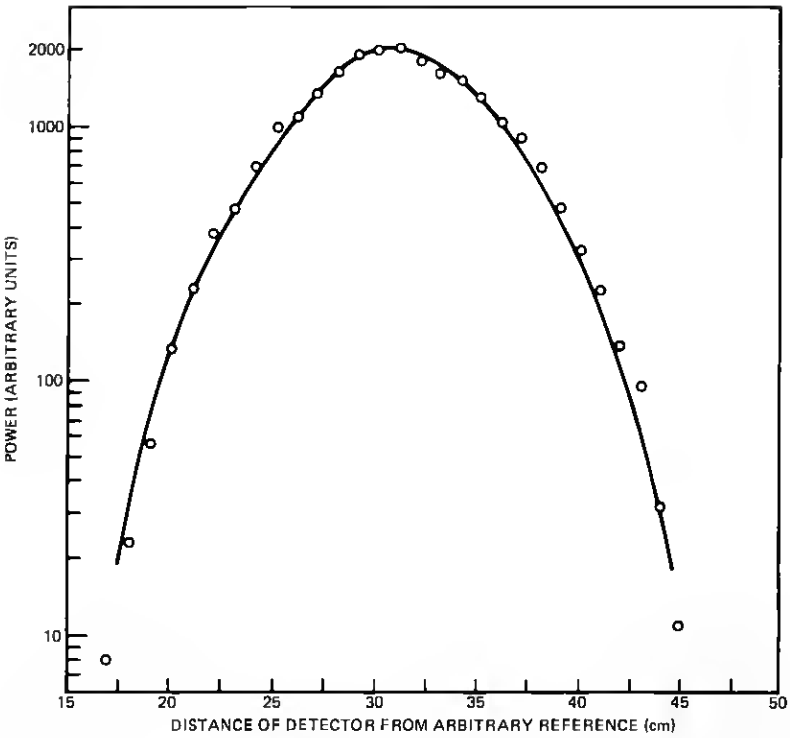

Fig. 3—Profile of beam in region between M1 and M2. The axis of the scan is perpendicular to the plane of the components in Fig. 2, and passes through the axis of the beam. Also shown is a gaussian beam with a beam half-width equal to 6.5 cm.

distance being only 140 cm indicates that this is an insignificant effect.

The difficulty in measuring the power distribution in the beam at the antenna beam waist can be overcome by utilizing the properties of a gaussian beam focused by lenses or mirrors; the beam half-width in the focal plane on one side of a converging lens with focal length f will be related to the beam-waist radius on the other side by[6]

$$\xi_{fp} = \frac{f}{k_o \xi_o} \tag{6}$$

In Fig. 3 we show a profile of the beam in the collimated region measured with a small-aperture (0.4 cm × 0.6 cm) horn and square-law detector. This measurement, which is well-fitted by a guassian with $\xi_1 = 6.5$ cm, together with eq. (6) confirms that the beam-waist size at 100 GHz is 1.0 cm, very close to the design value.

A signal passing through the Fabry-Perot resonator is focused by M2 into the feed horn attached to the mixer, located at the beam waist of

M2. The beam-waist radius at the feed horn is 0.32 cm at 100 GHz. The utilization of the Fabry-Perot with a diplexing angle of 8.5 degrees and M2 focal length equal to 44 cm requires that the dimension of M2 in the plane of the paper in Fig. 2 be approximately twice as large as would be required for focusing the signal beam alone.

The feedhorn for the receiver, which is the same design as that for the local oscillator, is a corrugated horn[7] with a beamwidth between −17 dB power points of 29 degrees. This type of feedhorn allows waveguide-bandwidth (90 to 140 GHz for the initial version) operation with high efficiency and very low sidelobes. For system tests performed at frequencies near 100 GHz we have, however, used relatively narrowband dual-mode horns[8,9] constructed in a manner similar to those described in Ref. 4. The power patterns are very similar to those of the corrugated horns, although with a beamwidth approximately 10 percent larger. All feed system characteristics refer to those measured with the dual-mode horns, but these should differ only in minor ways from those obtained with the corrugated horns.

2.4 Measurements of feed system efficiency

As discussed in the previous section, measurements of the power distribution in the collimated region indicate that the feed system will produce the correct taper in the illumination of the main antenna. In order to mesure the efficiency of the feed system, a separate collector was placed at the beam waist of M1, corresponding to the antenna beam waist. This collector, consisting of an ellipsoidal reflector and dual-mode feed horn, was independently measured to have a gaussian angular response pattern corresponding to a beam-waist size of 0.99 cm. A 100-GHz klystron with ~50 dB attenuation was used as a signal source. By interchanging a square law detector between the signal-source flange and the collector output flange (with the signal source connected to the feed system mixer flange), we determined the loss of power between the signal source and the collector output flange to be 1.1 dB. It should be noted that if part of this loss is due to the mode produced by the feed system not coupling to that accepted by the collector, this will not necessarily lower the efficiency when used with the antenna, but will only result in an illumination function slightly different from that anticipated. Thus the loss measured in this manner is an upper limit to the loss when used with an antenna. While the losses of the individual elements cannot easily be measured separately, the symmetry of the system suggests that half of the measured loss is due to the collector, and half is in the feed system, with a resulting feed system loss of 0.5 dB.

In Table I we summarize the salient characteristics of the feed system.

Table I — Feed system characteristics at 100 GHz

Characteristic	Value
ξ_1, collimated beam-waist radius to $1/e$ power point	6.5 cm
ξ_0, beam-waist radius to $1/e$ power point at antenna beam waist	0.97 cm
T_M, edge taper at main reflector	14.1 dB
θ_{FWHM}, full angular beamwidth to half-power points	1′.8
First sidelobe level relative to on-axis gain	−30 dB
ϵ_F, feed system loss (mixer waveguide flange to antenna beam waist)	0.5 dB
Spillover loss	0.14 dB
ϵ_M, beam efficiency	0.95

III. QUASIOPTICAL DIPLEXER

3.1 Introduction

The limited local-oscillator output power available at shorter millimeter wavelengths and the difficulty of fabricating low-loss waveguide diplexers[10] are incentives to seek an alternative to injection cavities and directional filters made in waveguide that are currently available. The use of a Fabry-Perot resonator as a diplexer is not new,[11,12] but the realization of a very low loss device to combine two signals differing in frequency by ~5 percent puts stringent restrictions upon the design of the resonator. There are a variety of configurations in which a Fabry-Perot resonator be used as a diplexer, e.g., with the signal in transmission or in reflection. A desirable characteristic of an ideal diplexer would be the ability to transmit power at the frequency of either one or both mixer sidebands. Single-sideband operation is important for accurate calibrations at millimeter wavelengths because the atmospheric attenuation in certain regions of the spectrum is a rapidly varying function of frequency.[13,14,15] Thus, although data analysis procedures have been developed which attempt to circumvent this problem,[16] the fact remains that an accurate determination of atmospheric extinction for spectral line work requires measurement of the attenuation in the sideband in which the line of interest is located. Also, the gain of a mixer receiver may well be different in the two sidebands, especially with the relatively high IF frequencies (4 to 5 GHz) that are now in use. For these reasons, systems have previously been devised which incorporate a Fabry-Perot resonator which either can be inserted in the optical path to measure the gain and attenuation in the two sidebands individually[17] or is permanently placed in front of the feed horn and which, at the expense of a small loss (~0.4 dB), suppresses the mixer response to the unwanted sideband.[18] In order to minimize the number of resonant elements and consequent adjustments required when changing frequencies, we decided

Table II — Characteristics of Fabry-Perot resonator at 100 GHz

T*	Image rejection ratio (dB)	0.5-dB bandwidth (MHz)	1-dB bandwidth (MHz)
0.10	26	220	320
0.15	22	350	500
0.20	19	540	800
0.25	17	620	890
0.30	15	760	1100
0.40	12	1090	1600
0.50	9.5	1500	2200

* T is the transmission of a single mirror.

to use the Fabry-Perot resonator in transmission for the signal (the local oscillator is reflected by the resonator, thus providing the diplexing action). This design allows us either to operate in a double-sideband mode with the two sidebands being transmitted in successive orders (for continuum work) or in a single-sideband mode (desirable for spectral line observations). Only one adjustment is required to set the diplexer for operation at a particular frequency, which proves to be a significant advantage in use.

3.2 Fabry-Perot resonator theory

The analysis of the propagation in a noninfinite Fabry-Perot resonator has been treated by Arnaud et al.[11] Since we will be dealing with a strongly tapered beam, it is sufficient to use the standard formulas for a plane wave in a resonator of infinite transverse dimension to calculate the response. Neglecting absorption in the mirrors, we find[19] that the fraction of the incident power transmitted by the resonator is given by

$$\tau = \frac{1}{1 + \dfrac{4(1-T)}{T^2} \sin^2 (k_o d \cos \theta)} \tag{7}$$

where d is the distance between the mirrors, θ is the angle from normal incidence of the radiation, T is the power transmission of a single mirror, and we have set the phase of the reflection coefficient equal to π which causes no loss of generality. In this limit we see that the peak transmission (for $k_o d \cos \theta = n\pi$, n being the order of operation) is equal to unity. The peak-to-valley ratio, or contrast factor, which will in our case be the image rejection ratio, and the 0.5-dB and 1-dB bandwidths for a resonator operating at 100 GHz are given in Table II as a function of T, which is assumed to be frequency-independent. It also has been assumed that the free spectral range of the resonator is approximately equal to 4 ν_{IF}; this is not a severe restriction since the transmission is only weakly dependent on frequency near the transmission minimum. There is a

tradeoff between bandwidth and image reflection, as expected for a simple resonator. This restriction could be eased by using a multiple-mirror resonator, but only at the expense of easy tunability. Efficient utilization of the bandwidth of available IF amplifiers (~600 MHz) indicates that T should not be less than 0.2; the resulting image rejection ratio of 19 dB is certainly adequate to assure proper calibration accuracy. It should be pointed out, however, that this ratio is not so high that the leakage of very strong lines from the opposite sideband in a high-sensitivity spectrogram can be entirely ruled out.

The Fabry-Perot diplexer exhibits quite high directivity for local oscillator injection. Power coming from the local oscillator feed horn that directly leaks thougb the Fabry-Perot resonator does not end up in the beam waist area at all, and is caugbt by a sheet of absorbing material. Only local oscillator power which is reflected from the Fabry-Perot, then reflected from the mixer feed horn, and which is finally transmitted by the resonator, can reach the calibration area; the level of this radiation should be at least 17 dB below that of the local oscillator power reaching the mixer.

The loss in a Fabry-Perot resonator operated at oblique incidence is primarily due to a walk-off effect in the finite-sized beam.[11] In this reference, the peak fractional transmission τ through a resonator (assumed to be much larger than the beam size) consisting of two mirrors of transmission T, spacing d, inclined at an angle θ to a gaussian beam of beamwaist radius ξ_o, is given by

$$\tau = 1 - G^2$$

where

$$G = \frac{2d \sin \theta}{\xi_o T} \tag{8}$$

For operation with $\nu_{IF} = 5$ GHz and $\nu_{SIGNAL} = 100$ GHz, obtaining the best image rejection ratio requires that the resonator be operated in fifth order so that $d = 5\lambda/2 = 0.75$ cm. The exact spacing will be determined by the resonance condition for the signal frequency; the condition $4\nu_{IF} = \nu_{SIGNAL}/5$ will be satisfied only approximately, but d will be close to the value given above. For $T = 0.2$ we find for small angles $\tau = 1 - (7.5\ \theta/\xi_o)^2$.

A lower limit on θ of $\sim 4/k_o\xi_o$ is found[11] from the condition that the beams be separable at the −17-dB level when the diffraction of each is considered. Thus the maximum transmission is (again for $T = 0.2$, $d = 0.75$ cm)

$$\tau_{MIN\theta} = 1 - \left(\frac{30}{k_o \xi_o{}^2}\right)^2 \tag{9}$$

As seen from eq. (8) the insertion loss, defined in decibels as $10 \log_{10} \tau^{-1}$, can, in theory, be made as low as desired, at the expense of enlarging the beam-waist radius. The beam waist required for low loss even in the optimum situation [eq. (9)] is moderately large; at $\nu = 100$ GHz and for the above conditions, $\xi_o = 2.6$ cm is required to achieve an insertion loss of 0.2 dB (the beam diameter will be at least $4\xi_o$). The most straightforward geometry (see, for example, Ref. 11) then results in a very large distance between the Fabry-Perot and the inputs for the signal and local oscillator; on the order of 1 meter for the above conditions. For this reason, and due to the simplicity of having the one mirror (M2) serve as collector for both the mixer and the local oscillator, the geometry of Fig. 2 was adopted. With a room temperature mixer, it would not be difficult to achieve a diplexing angle close to the theoretical minimum for a given loss, since the diameter of a dual-mode or corrugated feed is approximately 5 times the beam-waist diameter of the beam it launches. With a cryogenic receiver the minimum diplexing angle is set by the size of the dewar containing the mixer; we have used $\theta = 8.5$ degree (0.148 radian). To obtain an insertion loss of 0.15 dB the required beam-waist radius is approximately 6 cm; this number sets the size of the various mirrors and the focal length of M1, as well as the size of the Fabry-Perot resonator. The Fabry-Perot is shown in Fig. 4. In principle, one could utilize the minimum diplexing angle required for a given loss and collect the two spatially separated beams by mirrors which would refocus the beams wherever desired (i.e., into a dewar). This approach was not adopted because of alignment difficulties associated with the additional mirrors involved.

3.3 Measurements

3.3.1 Fabry-Perot mirrors

Each Fabry-Perot mirror consists of a photoetched copper mesh stretched on a metal support ring; the latter is similar to those described by Wannier et al.[18] The theory of one-dimensional wire grids[20] indicates that for the wires parallel to the electric field the grid behaves as a shunt inductance. We expect that a grid with square apertures will behave as a polarization-independent reflector as long as the angle of inclination of the incident beam is small.[21] For these grids with period $p = 1.07$ mm, strip widths $s = 0.29$ mm, and grid thickness $t = 0.08$ mm, one expects the relatively large value of t/s to decrease the equivalent inductance and thus decrease the transmission, compared to that of an infinitely thin grid.[20] The measured transmission at an incidence angle of 8.5 degrees is 0.19 ± 0.02 (at $\nu = 100$ GHz) compared to a transmission of 0.13 predicted theoretically; for an infinitely thin grid with the same aperture parameters, the theoretical transmission is 0.30.

Fig. 4—The Fabry-Perot resonator. The dial indicator on the right is used to monitor the mirror separation.

3.3.2 Fabry-Perot resonator

Examples of the frequency response of the Fabry-Perot resonator are shown in Fig. 5. These curves were obtained by sweeping a Siemens RWO 110B BWO connected to the mixer horn flange and monitoring the output from the collector located at the beam waist of M1. A measurement system consisting of a digitizer, log amplifier, and 1024 channel memory (Pacific Measurements model 1038) was used to first record the output without the Fabry-Perot. We then used this to correct the output measured with the Fabry-Perot in place for frequency-dependent variations in the oscillator output. The following parameters are obtained from these scans:

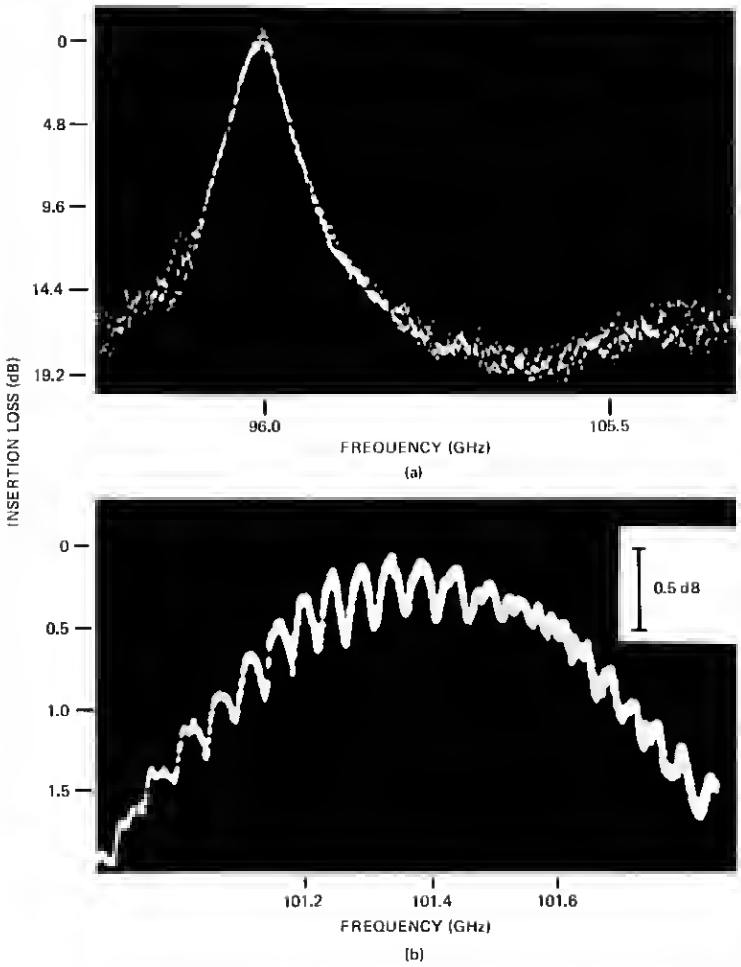

Fig. 5—(a) Transmission of the Fabry-Perot resonator as a function of frequency. The nominal value of 5 dB per vertical division was determined to be 4.5 dB from measurements with a precision attenuator. (b) Response near the transmission maximum, for a different mirror separation. Each vertical division corresponds to 0.5 dB. The ripple pattern is characteristic of the separation between the transmitter and receiver feed horns used in making the measurement.

$$\begin{aligned}&\text{Image rejection ratio} = 19\ \text{dB}\\&0.5\text{-dB bandwidth} = 510\ \text{MHz}\\&1\text{-dB bandwidth} = 780\ \text{MHz}\\&\text{Minimum insertion loss} = 0.25\ \text{dB}\end{aligned} \tag{10}$$

This last number is obtained by averaging over the ripple pattern in the central 250 MHz of the response pattern. The results presented here,

when compared to those given in Table II, indicate that the image rejection ratio measurement is consistent with a mirror transmission of 0.2, while the bandwidth measurements imply a transmission of about 0.21. The minimum resonator loss predicted by a mirror transmission of 0.2, $\theta = 8.5$ degrees, $\xi_o = 6.5$ cm, and $d = 0.75$ cm is 0.13 dB. If we allow for a loss of 0.12 dB from ohmic dissipation and/or other losses in the resonator, all of these measured characteristics are consistent within the errors with the expected resonator performance assuming a mirror transmission of 0.2.

3.3.3 Local oscillator loss

From the response curve of the Fabry-Perot (Fig. 5a), we see that the fraction of the local oscillator power leaking through the resonator will be only a few percent. If, for the moment, we consider the local oscillator injection process in reverse, we see that the mixer feed horn would produce essentially a plane wave heading towards M2, after reflection from the Fabry-Perot. In this case, the M2-local oscillator feedhorn combination should be considered as an off-axis offset parabolic antenna. The diplexing angle $\theta = 8.5$ degrees requires that the local oscillator feedhorn be 17 degrees or 24 half-power beamwidths off-axis. For a symmetric antenna with the same f/D ratio, the loss in gain would be less than 0.4 dB.[22] For an offset antenna, the theoretical loss is approximately 4 dB.[23] The measured loss for transmission between the flange of the local oscillator feed horn and that of the mixer feed horn is 2.7 dB. This is somewhat better than that achieved with a waveguide directional filter,[24] and far superior to results obtained with waveguide injection cavities.[25] If the diplexing angle were reduced by only a factor of two, the theoretical loss would be less than 1 dB.

3.3.4 Local-oscillator noise suppression

The Fabry-Perot diplexer as used here provides only 3 dB suppression of local oscillator noise since noise power at the image frequency is coupled into the mixer essentially as efficiently as power at the nominal local oscillator frequency. At an IF frequency of 5 GHz, a 3-dB filtering of the local-oscillator noise from a 100-GHz reflex klystron is sufficient to reduce the local oscillator noise to the equivalent of a 20 K input signal as measured with a single-ended mixer.[24] This is consistent with our measurements, in which we were unable to measure any increase in the diode noise temperature[26] using the Fabry-Perot diplexer, compared to using a high-Q injection cavity, with equal bias voltages and diode currents with the local oscillator on. In any case, local oscillator noise can easily be further reduced by a simple bandpass filter installed in the local oscillator waveguide.

3.3.5 Mixer performance

It is difficult to accurately measure the effect of the quasioptical diplexer on mixer performance, since most mixers when used with an injection cavity or directional filter are sensitive to signals in both sidebands, while with the Fabry-Perot resonator in its usual configuration the mixer in the quasioptical diplexer is sensitive to only one sideband. If we assume that the mixer is equally sensitive in the two sidebands, a comparison can be made. A room-temperature mixer with a transistor IF amplifier, when used with the quasioptical diplexer, was found to have an SSB noise temperature 0.7 dB better than that implied by a double-sideband measurement using an injection cavity diplexer. This same injection cavity was measured to have an insertion loss of 0.74 dB for the signal at 100 GHz while the quasioptical diplexer insertion loss is ~0.25 dB. The difference in noise temperatures is seen to be larger than the difference in diplexer losses, a fact which probably reflects the uncertainty in the relative response in the mixer sidebands. We do conclude, however, that the very low insertion loss for the quasioptical diplexer will probably be reflected in lower system noise temperatures.

3.4 Discussion

The Fabry-Perot diplexer described here exhibits low loss for the signal and for the local oscillator. The metal mesh mirrors actually had a lower transmission (0.2) than was expected (0.25) due to the larger thickness-to-aperture-size ratio compared to lower-frequency grids. Examination of Table II indicates that a mirror transmission of 0.27 might be optimum; this would lower the theoretical loss by a factor of 2. A more elaborate optical system would allow a diplexing angle at least 2 times smaller than that used, which would lower the loss by a factor of 4, or else would allow the beam and resonator diameters to be halved for the same loss. Thus it is seen that this technique has not been pushed to its limit in terms of low loss or compactness.

The use of the Fabry-Perot as a diplexer is also feasible in the submillimeter region. The techniques for making the mirrors are available and have been used to make resonators, operating at wavelengths between 80 μ and 600 μ.[19,27] If the ratio of the IF frequency to signal frequency is held constant, the order of operation of the resonator will remain fixed and the mirror separation will be proportional to the signal wavelength. Then, to obtain a given loss [eq. (8)], the beam size will also be proportional to the wavelength. If, on the other hand, a fixed IF frequency is used, the beam size required to obtain a given loss will be independent of the wavelength.

This quasioptical diplexer is also well suited to dual-polarization applications. The properties of the Fabry-Perot resonator are essentially

polarization independent. Thus, if the polarization angle of the local oscillator feedhorn is rotated 45 degrees to that of the mixer feedhorn, equal amounts of local-oscillator power would be detected in the two polarizations at the mixer feed horn. Either a dual-polarization feed horn or two feed horns with orthogonal polarizations fed by a wire-grid polarization splitter could be utilized.

IV. CALIBRATION SYSTEM

The calibration system shown in Fig. 6 is designed to provide a convenient method of measuring the receiver gain and atmospheric attenuation, and to allow various modes of observation. Each of these functions will be briefly discussed.

4.1 Receiver calibration

Not shown in Fig. 6 is a load consisting of truncated pyramids of Eccosorb* VHP-2 absorber which can be inserted into the beam that has passed from M1 through the rotary chopper. This provides a load at near ambient temperature. A cold load at liquid nitrogen temperatures has been constructed from pyramids of Eccosorb VHP-2 absorber in a dewar of liquid nitrogen. The index of refraction of liquid nitrogen is 1.4 at low frequencies[28] and should not be significantly higher at millimeter wavelengths. The resulting power reflection coefficient is 0.03. The power reflected by the absorber at the bottom of the dewar filled with nitrogen is measured to be approximately 20 dB below that reflected from a metal plate at the bottom of an empty dewar. We thus conclude that cold load is likely to be a moderately good calibration standard; its stability and emissivity have not been measured. By rotating the chopper (with the movable mirror out of the beam) a temperature difference of approximately 210 K is produced. It is possible that for very low noise receivers, this change in total power produced may exceed the limit allowable for good detector linearity. In this event, a calibrated, computer-controlled attenuator will be switched in synchronism with the chopper to keep the total power more nearly constant.

4.2 Measurement of atmospheric attenuation

This function is accomplished by chopping between the sky and either the ambient temperature or the cold load. The choice of reference depends on the sky temperature; the maximum temperature difference of ~100 K will probably be small enough to ensure good detection linearity. The atmospheric attenuation is then computed from an assumed

* Registered trademark of Emerson Cuming Inc., Canton, Mass.

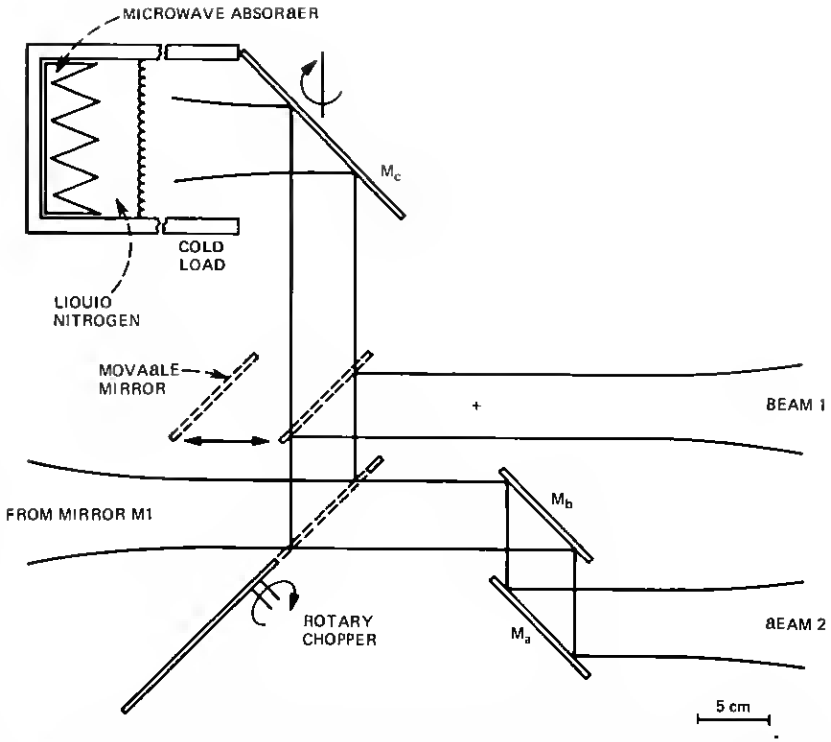

Fig. 6—The calibration system. The cross indicates the location of the antenna beam waist, while the lines shown approximate the −17 dB contours of the power distribution. The view presented is with the antenna pointing at zenith; at other elevation angles the cold load mirror M_c pivots about the axis indicated to keep the surface of the liquid nitrogen parallel to the horizon and perpendicular to the incident beam. Not shown is an ambient-temperature absorber that can be inserted between the chopper and M_b; its position, as well as that of the rotary chopper and movable mirror, is under computer control.

physical temperature (or temperature distribution) for the absorbing gas.

4.3 Beam switching

For observation of moderately small sources this technique is advantageous in that fluctuations in atmospheric emission will cancel if the chopping rate is sufficiently high and the scale size of the inhomogeneities is larger than the beam separation.[29] The separation between the two beams is 13′. This large value will be useful astronomically, but if the separation proves too large for effective noise cancellation, it can easily be reduced to about 6′. The uncertainty in the power spectrum of atmospheric fluctuations has led us to make the chopper speed variable between 2 Hz and 50 Hz. Observational experience will be required to determine the optimum chopping speed at different wavelengths under different atmospheric conditions.

V. SUMMARY

We have designed and tested a feed system for use with millimeter radio-astronomical receivers on a 7-meter Cassegrain antenna. We have measured that power incident on the mixer waveguide flange is transmitted to the antenna beam waist in the desired mode with a loss less than 1.1 dB and probably close to 0.5 dB. The antenna beam efficiency should be 0.95. The feed system incorporates a Fabry-Perot diplexer which has an insertion loss of 0.25 dB (transmission = 0.94) for a signal at 100 GHz and a loss of 2.7 dB for the local oscillator with a frequency differing by 5 GHz. A calibration system incorporates an ambient temperature load and a liquid nitrogen load, and a rotary chopper to switch between the two, between either one and tbe sky, or between two beams separated by 13′ on tbe sky.

The low loss and versatility of quasioptical techniques at millimeter wavelengths are expected to prove advantageous in obtaining well-calibrated high-sensitivity astronomical data.

ACKNOWLEDGMENT

I wish to thank J. Arnaud, T. S. Chu, A. A. M. Saleh, and R. W. Wilson for devoting considerable time to many helpful discussions about various aspects of this work. R. A. Linke supplied the mixer used in the tests, and also valuable information about mixer operation. Several coworkers at Crawford Hill generously made the results of their work available before publication. In particular, C. Dragone provided data on offset cassegrain antennas, M. J. Gans supplied data on truncated gaussian beams, and J. T. Ruscio made available the results of his measurements on mesh transmission. F. A. Pelow supervised making the metal mesh mirrors, R. A. Semplak supplied the collector used in measuring the feed-system efficiency, and W. Legg tuned and measured the patterns of the two feed horns. Thanks are also extended to R. L. Plambeck for a variety of helpful suggestions and to A. A. Penzias for encouragement to begin this project.

REFERENCES

1. C. Dragone and D. C. Hogg, "The Radiation Pattern and Impedance of Offset and Symmetrical Near-Field Cassegrainian and Gregorian Antennas," IEEE Trans. Ant. Propag., *AP-22*, May 1974, pp. 472–475.
2. J. A. Arnaud, *Beam and Fiber Optics*, New York: Academic Press, 1976, pp. 50–64.
3. J. D. Kraus, *Radio Astronomy*, New York: McGraw-Hill, 1966, pp. 154–159.
4. M. J. Gans and R. A. Semplak, "Some Far-Field Studies of an Offset Launcher," B.S.T.J., *54*, No. 7 (September 1975), pp. 1319–1340.
5. J. A. Arnaud, op. cit., pp. 74–79.
6. J. A. Arnaud, op. cit., pp. 65–67.
7. A. J. Simmons and A. F. Kay, "The Scalar Feed—A High Performance Feed for Large Parabolid Reflectors" in *Design and Construction of Large Steerable Aerials*, IEE Conf. Pub. 21, 1966, pp. 213–217.
8. P. D. Potter, "A New Horn Antenna Witb Suppressed Sidelobes and Equal Beamwidths," Microw. J., *6*, June 1963, pp. 71–78.

9. R. H. Turrin, "Dual Mode Small Aperture Antennas," IEEE Trans. Ant. Propag., *AP-15*, March 1967, pp. 307–308.
10. G. T. Wrixon, "Low-Noise Diodes and Mixers for the 1–2mm Wavelength Region," IEEE Trans. Microw. Theory Tech., *MTT-22*, December 1974, pp. 1159–1165.
11. J. A. Arnaud, A. A. M. Saleh, and J. T. Ruscio, "Walk-Off Effects in Fabry-Perot Diplexers," IEEE Trans. Microw. Theory Tech., *MTT-22*, May 1974, pp. 486–493.
12. J. A. Arnaud and F. A. Pelow, "Resonant Grid Quasi-Optical Diplexers," B.S.T.J., *54*, No. 2 (February 1975), pp. 263–282.
13. P. W. Rosenkranz, "Shape of the 5mm Oxygen Band in the Atmosphere," IEEE Trans. Ant. Propag., *AP-23*, July 1975, pp. 498–506.
14. C. J. Gibbins, A. C. Gordon-Smith, and D. L. Croom, "Atmospheric Emission and Attenuation in the Region 85-118 GHz," in *Conference on Propagation of Radio Waves at Frequencies Above 10 GHz*, IEE Conf. Pub. 98, 1973, pp. 132–140.
15. F. T. Ulaby, "Absorption in the 220 GHz Atmospheric Window," IEEE Trans. Ant. Propag., *AP-21*, pp. 266–269, March 1973.
16. J. H. Davis and P. Vandenbout, "Intensity Calibration of the Interstellar Carbon Monoxide Line at λ2.6 mm," Astrophys. Lett., *15*, September 1973, pp. 43–47.
17. R. L. Plambeck, D. R. W. Williams, and P. F. Goldsmith, "Comparison of $J = 2 \rightarrow 1$ and $J = 1 \rightarrow 0$ Spectra of CO in Molecular Clouds," Ap. J. (Letters), *213*, April 1, 1977, pp. L41–45.
18. P. G. Wannier, J. A. Arnaud, F. A. Pelow, and A. A. M. Saleh, "Quasioptical Band-Rejection Filter at 100 GHz," Rev. Sci. Instrum., *47*, January 1976, pp. 56–58.
19. R. Ulrich, K. F. Renk, and L. Genzel, "Tunable Submillimeter Interferometers of the Fabry-Perot Type," IEEE Trans. Microw. Theory Tech., *MTT-11*, September 1963, pp. 363–371.
20. N. Marcuvitz, *Waveguide Handbook*, New York: McGraw-Hill, 1951, pp. 280–289.
21. J. A. Arnaud and F. A. Pelow, opt. cit., pp. 262–264.
22. J. Ruze, "Lateral-Feed Displacement in Paraboloid," IEEE Trans. Ant. Propag., *AP-13*, September 1965, pp. 660–665.
23. C. Dragone, private communication.
24. B. D. Moore and J. R. Cogdell, "A Millimeter Wave Directional Filter Cavity," IEEE Trans. Microw. Theory Tech., *MTT-24*, November 1976, pp. 843–847.
25. R. A. Linke, private communication.
26. S. Weinreb and A. R. Kerr, "Cryogenic Cooling of Mixers for Millimeter and Centimeter Wavelengths," IEEE J. Solid State Circuits, *SC-8*, February 1973, pp. 58–63.
27. D. Brandshaft, R. A. McLaren, and M. W. Werner, "Spectroscopy of the Orion Nebula From 80 to 135 Microns," Ap. J., *199*, July 1975, pp. L115–L117.
28. R. C. Weast, ed., *Handbook of Chemistry and Physics*, Cleveland: CRC Press, 1975, pp. E55–E56.
29. J. W. M. Baars, *Dual Beam Parabolic Antennae in Radio Astronomy*, Groningen: Wolters-Noordhoff, 1970, pp. 59–116.